MAGNETIC RESONANCE IN MEDICINE **24,** 14–28 (1992)

Iron–Dextran as a Magnetic Susceptibility Contrast Agent: Flow-Related Contrast Effects in the T2-Weighted Spin-Echo MRI of Normal Rat and Cat Brain

DAVID L. WHITE, KLAUS P. AICHER, A. ARIA TZIKA, JOHN KUCHARCZYK, BARRY L. ENGELSTAD, AND MICHAEL E. MOSELEY

Department of Radiology, University of California, San Francisco, 513 Parnassus Avenue, San Francisco, California 94143

Received June 22, 1990; revised April 8, 1991

Iron–dextran (1 mmol Fe/kg) was used as an intravascular, paramagnetic contrast agent in rat and cat brain in conventional spin-echo T2-weighted (TR 2800/TE 100) ^{1}H magnetic resonance imaging. The resulting images displayed differential decreases (30–50%) in intensity whose pattern was similar to that obtained with the superparamagnetic particulate iron oxide AMI-25 (0.18 mmol Fe/kg). Postcontrast images displayed improved anatomic detail, and contrast effects were observed to be greater in cortical and subcortical gray matter than in adjacent white matter. Intravenous injection of acetazolamide after administration of iron–dextran caused a small additional decrease in image intensity. Measurement of whole blood and plasma at 5 min postinjection of either contrast agent revealed significant increases in their volume magnetic susceptibilities. The contrast effect appears to be related to magnetic susceptibility changes brought about by the iron–dextran; it has both blood volume and blood flow components. The static model of magnetic susceptibility effects in brain capillaries is modified to include bolus flow of erythrocytes, providing a mechanism for the observed flow effects.

INTRODUCTION

Villringer and co-workers (*1*) recognized that differences in magnetic susceptibility between the intracapillary space and surrounding tissue could provide a contrast mechanism in T2-weighted magnetic resonance imaging (MRI). Compartments with different magnetic susceptibilities experience different induced fields when placed in an external magnetic field, and protons diffusing through the resulting field gradients undergo spin dephasing (*2*), which causes loss of signal intensity. They observed transient signal intensity losses in normal rat brain with a rapid, one-dimensional projection spin-echo sequence after iv administration of diethylenetriaminepentaacetic acid (DTPA) complexes of Dy(III), Gd(III), or Pr(III) and attributed these results to magnetic susceptibility effects. These agents were effective in the brain since they cannot cross the blood–brain barrier and equilibrate in the extravascular space.

Majumdar *et al.* (*3*) observed contrast enhancement with a superparamagnetic iron oxide particulate agent (AMI-25) in the gradient-recalled-echo MRI of rat brain. They concluded that the contrast was due in part to magnetic susceptibility effects arising from the intracapillary contrast agent and diffusion of extracapillary water.

0740-3194/92 $3.00

We report herein similar susceptibility-based contrast enhancement in rat and cat brain following the iv injection of iron–dextran (Imferon), a drug that has long been clinically used for the treatment of iron deficiency. This paramagnetic ferric oxyhydroxy colloid has a very low acute toxicity (*4*). Thus relatively high doses can be used which, combined with its long plasma half-life, can compensate for its relatively low relaxivity and magnetic susceptibility per mole of iron.

The model of Villringer and co-workers (*1*) for magnetic susceptibility effects in capillary beds did not address the possibility of flow effects. In this paper, their model has been modified to incorporate the bolus flow of blood in capillaries. This change provides a magnetic susceptibility mechanism to account for observed blood flow effects on image signal intensity.

MATERIALS AND METHODS

Materials

Imferon (Merrell–Dow, Cincinnati, OH) or Proferdex (Fisons Corp., Bedford, MA) intravascular formulations of iron–dextran were used. Superparamagnetic particles (AMI-25) were obtained from Advanced Magnetics, Inc. (Cambridge, MA); Gd-DTPA was obtained from Schering, A.G. (Berlin); and acetazolamide was purchased from Lederle Laboratories Division (American Cyanamid, Inc., Wayne, NJ). Na_2Dy(DTPA) was prepared by refluxing equilmolar amounts of Dy_2O_3 (Alfa Inorganics, Bedford, MA) and DTPA as the free acid in aqueous suspension, followed by neutralization and filtration of the reaction mixture.

Magnetic Susceptibility Measurements

Susceptibility determinations were carried out using a S.H.E. Squid Magnetometer (S.H.E. Corp., San Diego, CA) at 37°C and 2.0 T. Liquid samples (100 μl) were measured in a screw-capped Kel-F container. Molar susceptibilities of Na_2Dy(DTPA), (meglumine)$_2$Gd(DTPA), iron–dextran, and AMI-25 in aqueous solution or suspension were corrected for container and solvent. Rat venous blood was withdrawn drawn from the jugular vein before and 5 min after injection of either iron–dextran (1 mmol Fe/kg) or AMI-25 (0.18 mmol Fe/kg) via a tail-vein catheter.

Relaxivity Measurements

Relaxation determinations were carried out at 37°C and 0.25 T on a Praxis Spectrometer (Praxis, Corp., San Antonio, TX) using a 90–τ–90 pulse sequence. The rate of disappearance of the contribution of contrast agent to venous blood T1 was determined from pre- and postcontrast samples taken at various time intervals.

Imaging

Imaging was performed on a CSI 2-T (85.6 MHz proton frequency) imaging spectrometer system (GE Medical Systems, Inc., Fremont, CA) equipped with GE Acustar S-150 self-shielding gradient coils. Distributed-capacitance volume-imaging RF coils,

5 and 10 cm i.d., were used for rat and cat imaging, respectively. Four-slice spin-echo T2-weighted images were acquired with the following parameters: TR 28000 ms; TE 100 ms; NEX 2; 3-mm slice thickness with 1-mm gap; 128 × 256 image matrix. The total acquisition time was 12 min. Fields-of-view were 60 × 60 mm and 81 × 81 mm for the rat and cat images, respectively. Subtraction images were generated by subtraction of the raw data sets, followed by data reconstruction.

Data Analysis

Region-of-interest (ROI) mean voxel signal intensity (SI) measurements were done on a Sun 3-160 computer (Sun Microsystems, Inc., Mountain View, CA) using Image software (New Methods Research, Inc., Syracuse, NY). Contrast enhancement was calculated according to the formula:

$$\% \text{ Enhancement} = 100 \times (SI_{pre} - SI_{post})/SI_{pre} \quad [1]$$

The animal-to-animal variations in SI were large relative to SI differences observed in individual animals as a function of time, in the presence of acetazolamide, or upon death. Therefore these differences were calculated for each animal according to the formula

$$\text{Difference} = (SI - SI_0)/SI_0, \quad [2]$$

where SI_0 and SI equal the signal intensities of an ROI before and after treatment. Mean differences and standard deviations were calculated, and the two-sided Student *t* test was used to test the hypothesis that the mean SI difference equaled zero.

Animals

Male Sprague–Dawley rats (250–300 g) were anesthetized ip with a mixture of ketamine (90 mg/kg) and diazepam (10 mg/kg), and anesthesia was maintained with pentobarbital (15 mg/kg) given via an intraperitoneal catheter. Each animal was fitted with a catheter in a lateral tail vein through which contrast agent was administered.

Mixed breed cats ($n = 2$) were anesthetized with sodium pentobarbital (30 mg/kg iv) and fitted with arterial and venous catheters.

Imaging Protocols

Normal animals were imaged using the T2-weighted sequence before and at 0, 15, and 30 min postinjection of either iron–dextran ($n = 4$ rats, 2 cats; 1.0 mmol Fe/kg) or AMI-25 ($n = 4$ rats; 0.18 mmol Fe/kg). Each animal then was euthanized with a lethal dose (100 mg/kg) of pentobarbital, and a postmortem image was immediately obtained.

An additional set of rats ($n = 4$) was imaged as above without injection of iron–dextran in order to observe post–pre mortem intensity changes in the absence of contrast agent.

A group of rats ($n = 4$) was imaged with iron–dextran as above, except that acetazolamide (100 mg/kg) was administered iv 30 min after the contrast agent injection.

An image then was obtained 15 min later (45 min postcontrast). Each animal then was euthanized as above, and an immediate postmortem image was obtained.

An acetazolamide control group of rats ($n = 4$) was treated as described immediately above, except the iron–dextran injection was omitted.

RESULTS

Relaxivity

The R1 and R2 of Imferon in water at 37°C and 0.25 T were 1.6 and 3.4 $mmol^{-1}$ s^{-1}, respectively. The contribution of Imferon (1.0 mmol Fe/kg) to venous blood T1 decreased monoexponentially with a half-life of 12.6 h. AMI-25 (0.18 mmol/kg) displayed a biexponential clearance with 16.6 min (49%) and 84.5 min (51%) half-lives. Majumdar and co-workers (*3*) observed $t_{1/2}$'s of image intensity recovery of 9.2 and 15 min for doses of 0.07 and 0.14 mmol Fe/kg, respectively.

Magnetic Susceptibility

The molar susceptibilities at 37°C and 2 T of $(meglumine)_2Gd(DTPA)$, $Na_2Dy(DTPA)$, Imferon, and AMI-25 are given in Table 1.

Iron–dextran at a dose of 1 mmol Fe/kg caused a significant positive (i.e., paramagnetic) change in the volume magnetic susceptibilities of both whole blood and plasma at 5 min postinjection (Table 2). This is consistent with the blood hematocrit and the observation from relaxivity data (*vide infra*) and radiotracer studies (*4*) that iron–dextran initially distributes in the blood plasma.

Since the volume susceptibility of a mixture is the sum of the volume susceptibilities of each component multiplied by the volume fraction of that component (*5*), the susceptibilities of Imferon and pre- and postinjection blood were used to calculate the blood volume and confirm the accuracy of the measurements. The values given in Table 2 are in excellent agreement with literature value of 64.1 ml/kg (*6*).

TABLE 1

Magnetic Properties of Contrast Agents

	Molar susceptibility χ_M (emu)	Magnetic moment[a] (Bohr magnetons)	M(III) spin only magnetic[b] moment (Bohr magnetons)
Iron–dextran[c]	1.31×10^{-2}	5.72	5.9
$Meglumine_2[Gd(DTPA)]$	2.55×10^{-2}	7.98	7.9
$Na_2[Dy(DTPA)]$	3.67×10^{-2}	9.58	10.6
AMI-25[c]	1.77×10^{-1}		

[a] $m = 2.84(\chi_M T)^{1/2}$.

[b] J. C. Bailar, H. J. Emeleus, R. Nyholm, and A. F. Troman-Dickenson, Eds., "Comprehensive Inorganic Chemistry," Pergamon Press, Oxford, 1973.

[c] Per mole Fe.

TABLE 2

In Vivo Magnetic Susceptibility Data

Agent	Animal No.	Wt (g)	Inj vol (ml)	Hematocrit	Blood volume magnetic susceptibility χ_v (emu × 10^6)				Plasma volume magnetic susceptibility				Calculated[b] RBC χ_v (emu × 10^6)	Calculated[c] blood vol (ml/kg)
					Pre	Post	Difference	$\Delta H/H$[a] (ppm)	Pre	Post	Difference	$\Delta H/H$[a] (ppm)		
Iron–dextran	1	248	—	0.41	−0.751	−0.433	0.318	1.33	−0.737	−0.276	0.461	−1.16	−0.771	—
	2	243	0.27	0.37	−0.737	−0.536	0.207	0.87	−0.716	−0.318	0.398	−1.33	−0.789	65.7
	3	234	0.26	0.50	−0.697	−0.484	0.213	0.89	—	—	—	—	—	63.6
AMI-25	1	252	0.22	0.51	−0.725	−0.266	0.459	1.92	−0.716	0.288	1.004	1.21	−0.734	[d]
	2	250	0.22	0.50	−0.729	−0.377	0.352	1.47	−0.704	0.442	1.146	1.85	−0.754	[d]
	3	235	0.21	0.50	−0.717	0.210	0.927	3.88	−0.706	2.740	3.446	11.48	−0.728	[d]

[a] $(-4\pi/3)\chi_v$. (Ref. (7)).

[b] $\chi_{v(RBC)} = [\chi_{v(Blood)} - (H - 1)\chi_{v(Plasma)}]/H$, where H = hematocrit.

[c] Blood vol = [(inj vol) × $(\chi_{v(Contrast\ agent)} - \chi_{v(Post\ blood)})$]/[$(\chi_{v(Post\ blood)} - \chi_{v(Pre\ blood)})$].

[d] Not calculated. The concentration of AMI-25 changed significantly over 0–5 min postinjection.

The change in field experienced by postcontrast blood in vessels was estimated using the dependence of chemical shift upon bulk magnetic susceptibility. A cylindrical sample of effectively infinite length with perpendicular or parallel orientation to the applied field will experience bulk susceptibility contributions to the chemical shift $\sigma_b^{\perp}$ or $\sigma_b^{\parallel}$ that are given by the equations (*7*):

$$\sigma_b^{\perp} = 2/3\pi\chi_v \quad [3]$$

or

$$\sigma_b^{\parallel} = -4/3\pi\chi_v \quad [4]$$

Thus the maximum change in field experienced by blood containing iron–dextran should be −1.3 ppm, or −0.026 Gauss at 2 T (see Table 2).

The root mean square displacement, χ, for isotropic diffusion of water during a time t is given by

$$\chi = (2Dt)^{1/2}, \quad [5]$$

where D is the diffusion constant. Apparent diffusion constants of $0.25–2.0 \times 10^{-9}$ m^2/s for water in the brain have been reported (*8, 9*). Substituting these for D, and 0.1 s = TE = t, one obtains a range of 7–20 μm for χ. If the field difference at the capillary surface is 0.026 Gauss (see above), the average field gradient experienced over the distance χ from the capillary surface is 0.026 Gauss/13.5 μm, or 19 Gauss/cm.

Note that the calculated values for χ approximate one-half of the average intercapillary distance of 23.4 μm (*1*), and thus most of the extravascular water protons should be subject to a significant field gradient.

Imaging

Iron–dextran at 1 mmol Fe/kg caused the overall enhancement of normal rat brain to fall by 30–50% (Fig. 1 and Table 3). However, this loss of signal intensity was not uniform over all regions of the brain, with regions of higher blood flow (cortical and subcortical gray matter) appearing more hypointense than adjacent white matter. The pre–post subtraction image clearly demonstrates the heterogeneity of the contrast effect (Fig. 1c).

Similar results were also obtained in normal cat brain, where the larger size and greater complexity of the cortical gyri could be clearly seen (Fig. 2). In one experiment, the animal became severely hypotensive and died after the bolus injection (over 30 s) of iron–dextran. The second experiment was successfully carried out with slow injection (3 min) of the contrast agent as the blood pressure was monitored (see Ref. (*10*)).

The hypothesis that the iron–dextran contrast effects arise from magnetic susceptibility gradients is supported by the parallel enhancement results obtained with the superparamagnetic particulate AMI-25 (Table 3). The pre- versus postcontrast rat brain images are strikingly similar (cf. Figs. 1 and 3), presumably because similar contrast mechanisms are operative.

Rat brain SI increased ca. 25–30% upon euthanasia (Table 4) when iron dextran or AMI-25 was present. Without contrast agent, the increase in SI was considerably

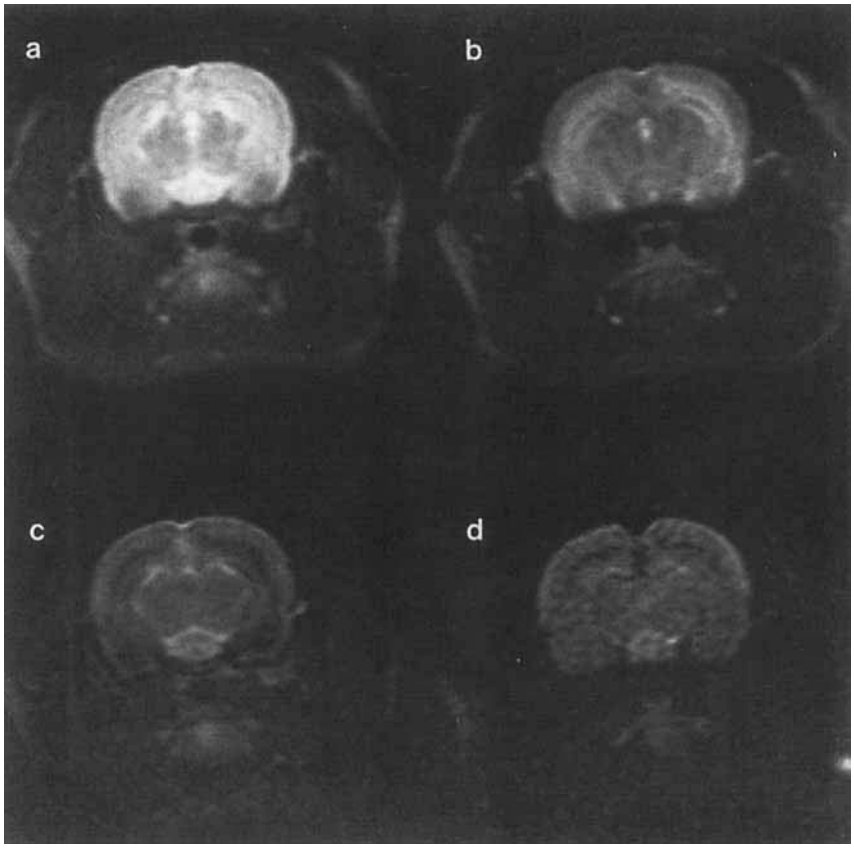

FIG. 1. T2-weighted (TR/TE = 2800/100) coronal images of a rat brain at the level of the hypothalamus (3-mm slice; FOV 60 mm) before (a) and immediately after (b) injection of iron–dextran (1 mmol Fe/kg). Cortical and subcortical gray matter appears hypointense relative to white matter because of higher CBF to gray matter. Lowest signal intensities are observed in the carotid arteries and midsagittal sinus. CSF in the anterior third ventricle is hypointense, presumably reflecting diffusion-related signal loss. Regional contrast effects are illustrated in the post–pre contrast subtraction image (c). The post–pre mortem subtraction image indicates flow-related changes in SI.

smaller (4–8%), but still statistically significant (Table 4). This change includes any effects of motion, as well as susceptibility effects of unenhanced blood (see Discussion).

Rat CSF intensities increased to a lesser extent with contrast agent present (Table 4). Although CSF pulsations and flow would cease immediately following death, dephasing arising from unrestricted CSF diffusion would be unchanged. Relatively small CSF ROI's and volume averaging effects resulted in higher variances for these measurements. Thus the observed mean post–pre mortem CSF SI difference was not statistically significant ($P < 0.10$).

Muscle intensities also increased (Table 4), but the absolute SIs were relatively low, and this contributed to its higher variance.

TABLE 3

Postcontrast Percentage of Enhancement in Normal Rat Brain (Mean ± SD; $n = 4$)

Agent and time postinjection	Cortex	Basal ganglia	Hemisphere	CSF	Muscle
Iron–dextran					
0 min	−36 ± 12	−39 ± 9	−40 ± 6	−48 ± 15	−33 ± 6
30 min	−32 ± 7	−36 ± 7	−33 ± 6	−39 ± 15	−20 ± 10
Postmortem	−14 ± 10	−16 ± 9	−20 ± 6	−33 ± 8	−5 ± 15
Iron–dextran and acetazolamide					
5 min	−24 ± 8	−32 ± 11	−27 ± 10	−35 ± 15	−27 ± 17
45 min (15′ post acetazolamide)	−27 ± 8	−36 ± 11	−30 ± 8	−38 ± 12	−19 ± 20
Postmortem	−18 ± 12	−25 ± 13	−22 ± 12	−28 ± 16	−27 ± 11
AMI-25					
0 min	−60 ± 6	−66 ± 4	−63 ± 6	−74 ± 4	−67 ± 4
30 min	−38 ± 10	−44 ± 10	−41 ± 11	−45 ± 12	−47 ± 11
Postmortem	−24 ± 5	−29 ± 5	−28 ± 6	−37 ± 7	−30 ± 24

Acetazolamide, which increases cerebral blood flow (CBF) (*11*) and to a lesser extent volume (*12*), caused no change in image SI in the absence of iron–dextran. When contrast agent was present, however, a statistically significant 5–7% decrease was observed (Table 4).

The plasma half-life for iron–dextran noted above suggested that the contrast agent concentration should decrease no more than 3% during the 15- to 30-min time period between image acquisitions. Consistent with this, the changes in SI observed during the first 30-min postinjection were not significant (Table 4). These results also suggest that the pre- minus postmortem changes cannot be explained by changes in iron–dextran concentration, but are due to cessation of blood flow or other physiologic motion and/or blood volume changes (see Discussion).

The plasma clearance data for AMI-25, however, predict a 46% fall in concentration over 30 min, and an additional 11% decrease from 30 to 45 min postinjection. The image SI of brain, CSF, and muscle increased from 50 to 100% during the 30 min immediately postinjection (Table 4). The SI changes of 23 to 28% from the last alive image (at 30 min pi) to the postmortem image (at 45 min pi) appears to be greater than can be explained by changes in contrast agent concentration alone. These results are consistent with the observations obtained with iron–dextran (see above).

DISCUSSION

Iron–dextran is prepared by the precipitation of a ferric salt in a alkaline solution of dextran (typically, MW = 5000). It is a paramagnetic, stable ferric oxyhydroxy colloid with particles of approximately 11 μm diameter containing an inorganic core approximately 3 μm in diameter (*13–15*). Both iv and im parenteral formulations (Imferon or Proferdex) containing 50 mg Fe/ml are available.

The magnetic susceptibility values in Table 1 indicate that iron–dextran is inferior in this respect to DTPA complexes of (paramagnetic) Dy(III) or Gd(III), or super-

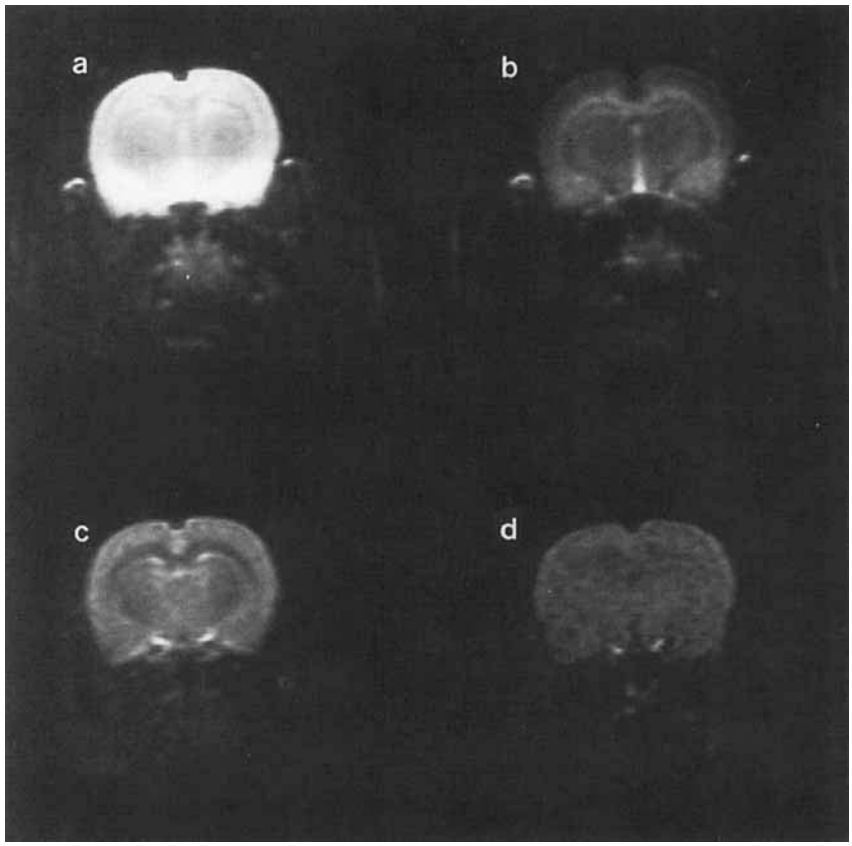

FIG. 2. T2-weighted (TR/TE = 2800/100) coronal image of rat brain before (a) and immediately after (b) injection of AMI-25 (0.18 mmol Fe/kg). Cortical and subcortical gray matter appear hypointense relative to white matter. In the pre–post contrast subtraction image (c), white matter (corpus callosum and internal capsule) has a lower signal intensity. The post–pre mortem subtraction image (d) shows regional differences in signal intensities, presumably reflecting flow effects.

paramagnetic iron oxide particles. However, the susceptibility agent must remain in the blood throughout the image acquisition for its full contrast effect to be observed. The low-molecular-weight lanthanide chelates have plasma clearance half-lives (*16*) that are comparable to the time required for T2-weighted spin-echo image acquisition; thus the observed average concentrations of these extracellular volume agents can be significantly lower than their initial concentrations. The same is true for the superparamagnetic iron oxide particulate AMI-25, which is cleared rapidly by the reticuloendothelial system (RES) (*3, 17*).

Iron–dextran is advantageous in that it is intravascular, even in tissues other than brain. Its plasma concentration remains essentially unchanged for time periods well in excess of those required for T2-weighted image acquisition. Although its molar

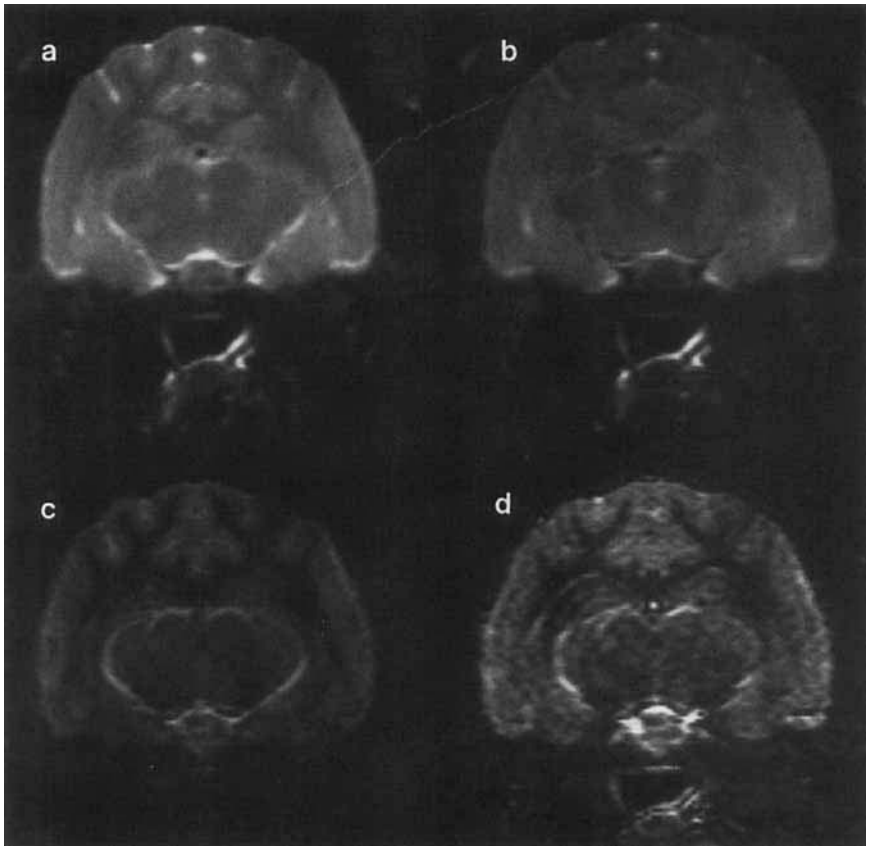

FIG. 3. T2-weighted coronal image (a) of a cat brain (3-mm slice; FOV 81 mm) at the level of the mesencephalon shows lowest SI for subcortical white matter (corpus callosum, corona radiata), high SI in CSF spaces, and intermediate SI for cortical and subcortical gray matter. Injection of iron–dextran (1 mmol Fe/kg) caused a loss of SI (b) in gray matter, which is especially well seen in the superior and middle parietal gyri and periacqueductal reticular formation. The post–pre contrast subtraction image (c) highlights gray–white matter signal differences. The post–pre mortem subtraction indicates changes in SI apparently due to blood flow.

susceptibility is relatively low, it is very soluble (~ 1 *M* [Fe]) and nontoxic ($LD_{50} >$ 18 mmol Fe/kg, iv in mice (*4*)). These two properties are remarkable, given the low solubility (log solubility = −41.5 at pH 7.4 (*18*)) and high toxicity (LD_{50} = 0.04 mmol Fe/kg iv in rabbits) of aquo Fe(III) (*19*).

Since the contrast effect is based upon bulk susceptibility ("long range" effects and spin dephasing of protons moving relative to the field gradient in the vicinity of capillaries) it is clear that the contrast effect of iron–dextran (or any other intravascular susceptibility agent) depends upon tissue blood volume. In addition to the blood volume effect, however, there also appears to be a significant blood flow component to observed

TABLE 4

Percent Differences in ROI Intensities in Rat Brain (Mean ± SD; $n = 4$)

Agent and time postinjection	Cortex	Basal ganglia	Hemisphere	CSF	Muscle
Iron–dextran					
30′–0′	8 ± 6	7 ± 3	12 ± 6	18 ± 10	20 ± 4
Postmortem–30′	26 ± 6*	32 ± 5*	25 ± 5*	17 ± 10	18 ± 9
Control					
Postmortem–premortem	5 ± 2**	8 ± 1*	4 ± 2**	−3 ± 2	−17 ± 9
Iron–dextran and acetazolamide					
Post–Pre acetazolamide	−5 ± 2**	−7 ± 3**	−5 ± 1*	−6 ± 5	12 ± 6
Acetazolamide control					
Post–Pre acetazolamide	0 ± 2	2 ± 3	0 ± 2	−6 ± 4	8 ± 9
AMI-25					
30′–0′	54 ± 6*	64 ± 8*	60 ± 5*	100 ± 8*	61 ± 14*
Postmortem–30′	23 ± 7*	28 ± 7*	25 ± 7*	25 ± 11	31 ± 14

* $\mu \neq 0$, $P < 0.05$.
** $\mu \neq 0$, $P < 0.1$.

signal intensity changes. This latter conclusion is based on the SI increase observed between pre- and immediately postmortem images using iron–dextran or AMI-25.

Physiologic changes that occur within a few minutes following cardiopulmonary arrest include temperature decrease, blood pooling, edema, blood volume changes, and cessation of breathing and blood flow. Although the first three may affect imaging, the changes in them that occur during the first 12 min (the image acquisition time) following death are probably not significant. No obvious image SI gradients, such as might be expected with heat loss or blood pooling, were observed; and subsequent images (e.g., from about 15 to 25 min following death) showed no additional changes. The small postmortem SI increases observed in these T2-weighted images in the absence of contrast media (Tables 3 and 4) suggest that edema was not a important factor.

It seems unlikely that changes in cerebral blood volume (CBV) could account for the postmortem SI increase. This would require a reduction by a factor of about two in the CBV upon death. Although blood pressure falls in the absence of cardiac output, the brain and heart were at essentially the same level in the supine rat, and there should have been no hydrostatic pressure gradient that would have resulted in outflow of blood or influx of tissue water.

Physiologic motion other than blood flow, e.g., pulsations or breathing, also appear to be relatively unimportant. This conclusion is based on the small SI increases observed upon death in the control experiments without contrast agent (Tables 3 and 4).

The results of the control experiments also indicate that any postmortem conversion of diamagnetic hemoglobin to paramagnetic dexoyhemoglobin is not dominant. Such a change would increase microscopic field gradients, causing additional dephasing and signal loss. Instead, the signal intensity increased slightly in the absence of contrast agent.

Thus the 25–30% increase in brain SI observed upon death appears to be largely due to cessation of blood flow. The decrease in intensity observed after injection of acetazolamide is consistent with this hypothesis, as it has been shown to cause up to 70% increases in CBF (*11*). However, acetazolamide also causes CBV to increase slightly (*12*), and this change should also result in a decrease in signal intensity in the presence of a magnetic susceptibility contrast agent.

A model based on bolus flow in capillaries has been developed to explain the loss of signal intensity related to flowing blood containing a magnetic susceptibility agent. The original model of Villringer and co-workers (*1*) relating susceptibility differences to SI explicitly assumed that capillaries were infinitely long cylinders and implicitly assumed that they were filled with a homogeneous medium of different volume susceptibility than that of the extracapillary space. Thus the field gradients due to a given capillary were radially symmetric and time invariant.

Villringer and co-workers (*1*) estimated that ca. 60% of the protons experienced significant field gradients using the following parameters: 1 ppm difference in intra- and extracapillary magnetic susceptibility; 2.5×10^{-10} m^2/s brain water diffusion coefficient; 2.3 μm average capillary radius; and 24 μm average brain intercapillary distance. This result is not inconsistent with the contrast effects observed under conditions of unaltered blood flow (*1, 3*), or with our observations and calculations.

However, consideration of the composition and flow of capillary blood can provide a mechanism to explain magnetic susceptibility contrast flow effects. Due to the relative size of capillaries (ca. 5 μm diam), and erythrocytes (ca. 7 μm diam $\times$ 2 μm thick), the capillary contents are not homogeneous. At this level of vasculature, flow becomes heterogeneous ("bolus flow"), with single-file passage of deformed erythrocytes separated by plasma segments ("interbolic plasma") (Fig. 4) (*20*).

The volume susceptibility of an erythrocyte depends upon the degree of hemoglobin oxygenation, ranging from approximately that of plasma or surrounding tissue (ca. -0.7×10^{-6} emu) for one with fully oxygenated hemoglobin to a somewhat more paramagnetic value (-0.5×10^{-6} emu) for an erythrocyte containing deoxyhemoglobin (*21*). Differences between these values and postcontrast plasma can be considerably greater ($\Delta\chi_v = 0.2\text{–}3.4 \times 10^{-6}$ emu), depending upon the type and dose of contrast

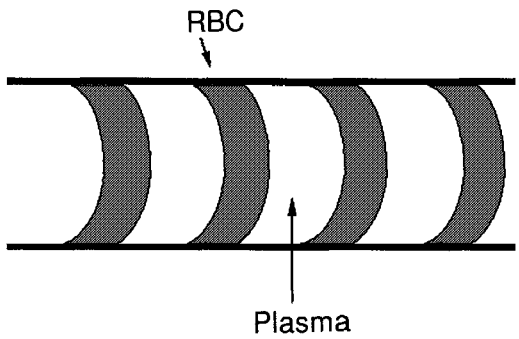

FIG. 4. Schematic diagram of bolus blood flow in a capillary showing erythrocytes and interbolic plasma.

agent (Table 2). Thus the capillary blood stream can be thought of as a series of low susceptibility "bubbles" separated by liquid with approximately the same (plasma), or considerably greater (postcontrast plasma) magnetic susceptibility. These discontinuities can cause proportional field gradients within the capillary volume as well across the capillary endothelium boundary.

Packer (*22*) analyzed the diffusion of protons through periodic local field gradients based on the work of Robertson (*23*). Thulborn and co-workers (*21*) extended this treatment to *in vitro* blood. In it, the correlation time ξ for periodic diffusion is given by the equation

$$\xi_{\text{diff}} = (r_p)^2/2D, \qquad [6]$$

where r_p is the periodicity of the field gradient and D is the water diffusion coefficient. The periodicity in our model is the spacing of erythrocytes in the capillaries. Given that the capillary hematocrit is 30–40% of the systemic hematocrit (*20*), this spacing is probably in the range of $2\text{–}10 \times 10^{-6}$ m. Values of $0.25\text{–}2 \times 10^{-9}$ m^2/s have been reported (*8, 9*) for the diffusion coefficient of water in brain tissue. Substituting these values in Eq. [6] yields correlation times in the range of $1\text{–}200 \times 10^{-3}$ s.

The same analysis can be applied to the situation of a *stationary* proton and a *moving* field arising from the bolus flow of erythrocytes in capillaries. Since the root mean square diffusion velocity of brain water (χ/t from Eq. [5]) is $0.7\text{–}2 \times 10^{-4}$ m/s, a fraction of the capillary blood velocity ($v_{\text{rbc}} = 0.2\text{–}2 \times 10^{-3}$ m/s) (*20*), the approximation of a "stationary" proton is not unreasonable. In this case the periodicity is related to v_{rbc} and the thickness (*20*) of erythrocyte and interbolic plasma phases (Fig. 1). Substituting capillary blood velocities (*20*) and values of spacing (r_p) noted above in the equation

$$\xi_{\text{flow}} = r_p/v_{\text{rbc}} \qquad [7]$$

yields correlation times in the range $1\text{–}50 \times 10^{-3}$ s.

Thus the diffusion and bolus-flow correlation time ranges overlap, but it remains to be shown that processes with such correlation times can produce signal intensity effects such as those observed in our experiments.

Glasel and Lee (*24*) and Packer (*22*) have studied the effect of locally inhomogeneous magnetic fields on transverse relaxation times based on Robertson's (*23*) analysis of spins diffusing in a bounded region. Under the limiting condition that

$$\text{TE} \gg 2(r_p)^2/(\pi^2 D), \qquad [8]$$

where r_p is the spacing of the inhomogeneity and D is the diffusion coefficient, Parker derived an equation for the attenuation factor $R(\text{TE})$ in a $90\text{–}\tau\text{–}180$ SE sequence.

$$R(\text{TE}) \approx \exp - \{[(\Delta\omega)^2\xi/30][\text{TE}/2]\}, \qquad [9]$$

where $\Delta\omega$ is the spread of precession frequencies of the spins and ξ is the correlation time.

The results in Table 2 indicate that $\Delta\omega$ is about 1 ppm, or about 10^2 s^{-1} at 2 T. Substituting this value, the TE value of 10^{-1} s, and the diffusion and bolus-flow correlation times calculated above, one obtains $R(\text{TE})$ values in the range 0.43 to 0.99.

The results of control experiments (Table 4) suggest that of the 26–32% increase in SI upon death in animals given iron–dextran, about 20% was due to the presence of the contrast agent. Likewise, about one-half of the 40% decrease in postcontrast signal intensity (Table 4) is probably due to non-flow-related T2* effects, i.e., to diffusion. Thus the bolus-flow-related and the diffusion-related attenuation factors due to magnetically inhomogeneous blood are both approximately 0.8. This value, along with the $\Delta\omega$ and TE values used above, can be substituted into Eq. [9] to calculate a value of 1.3×10^{-2} s for both ξ_{diff} and ξ_{flow}. These values lie within the ranges calculated above using literature values for diffusion, flow, and spacing parameters.

CONCLUSIONS

Iron–dextran is a long-lived, intravascular contrast agent that can provide additional structural detail in the T2-weighted MRI of normal brain. The required dose is 10- to 20-fold larger than the maximum recommended clinical dose, and this may limit its application to animal experiments. However, a smaller dose may be required with techniques having a greater sensitivity to magnetic susceptibility effects (e.g., asymmetric-echo, gradient-recalled-echo, or echo-planar sequences).

The experimental results are consistent with a T2* mechanism of contrast enhancement. The presence of the intravascular paramagnetic contrast agent causes local changes in magnetic susceptibility that give rise to magnetic field gradients around capillaries. The relative motion of protons with respect to these fluctuating local gradients causes spin dephasing and concomitant loss of signal intensity.

This relative motion can arise in two ways: (1) diffusion of protons in the extracapillary space; and (2) bolus flow through the capillaries of volumes of different magnetic susceptibilities (and thus different fields). The latter correspond to erythrocytes and to plasma containing contrast agent. The estimated correlation times (about 13 ms) of these two processes are comparable, providing an explanation for the partial recovery of image intensity observed in immediate postmortem contrast-enhanced T2-weighted images.

ACKNOWLEDGMENTS

The authors thank Michael Wendland, Ph.D., for helpful discussions. The AMI-25 was a gift from Advanced Magnetics, Inc. The magnetic susceptibility measurements were carried out at the Lawrence Berkeley Laboratory, University of California—Berkeley, with the assistance of George Shalimoff and N. E. Edelstein. This research was supported by NIH Grant No. 1 RO1 CA 39818-05.

REFERENCES

1. A. VILLRINGER, B. R. ROSEN, AND J. W. BELLIVEAU, *et al., Magn. Reson. Med.* **6,** 164 (1988).
2. H. Y. CARR AND E. M. PURCELL, *Phys. Rev.* **94,** 630 (1954).
3. S. MAJUMDAR, S. S. ZOGHBI, AND J. C. GORE, *Magn. Reson. Imaging* **6,** 611 (1988).
4. L. GOLDBERG, in "Iron in Clinical Medicine" (R. O. Wallerstein and S. R. Mettier, Eds.), p. 74–92, Univ. of California Press, Berkeley, CA, 1958.
5. P. S. SELWOOD, "Magnetochemistry," 2nd ed., pp. 107–109, Interscience, New York, 1956.
6. H. J. BAKER, J. R. LINDSEY, AND S. H. WEISBROTH, in "The Laboratory Rat," Vol. 1, p. 411, Academic Press, New York, 1979.
7. J. K. BECONSALL, G. D. DAVES, AND W. R. ANDERSON, JR., *J. Am. Chem. Soc.* **92,** 430 (1970).

8. J. R. HANSEN, *Biochim. Biophys. Acta* **230,** 482 (1971).
9. D. LEBIHAN, E. BRETON, D. LALLEMAND, M. L. AUBIN, J. VIGNAUD, AND M. LAVAL-JEANTET, *Radiology* **168,** 497 (1988).
10. J. S. G. COX AND R. E. KING, *Nature* **207,** 1202 (1965).
11. S. COTEV, J. LEE AND J. W. SEVERINGHAUS, *Anesthesiology* **29,** 471 (1968).
12. P. E. BICKLER, L. LITT, AND J. W. SEVERINGHAUS, *J. Appl. Physiol.* **65,** 428 (1988).
13. C. R. RICKETTS, J. S. G. COX, C. FITZMAURICE, AND G. F. MOSS, *Nature* **208,** 237 (1965).
14. P. R. MARSHALL AND D. RUTHERFORD, *J. Coll. Inter. Sci.* **37,** 390 (1971).
15. L. JOSEPHSON, J. LEWIS, P. JACOBS, P. F. HAHN, AND D. D. STARK, *Magn. Reson. Imaging* **6,** 647 (1988).
16. R. C. BRASCH, H-J. WEINMANN, AND G. E. WESBEY, *Am. J. Roentgenol.* **142,** 625 (1984).
17. R. WEISSLEDER, D. D. STARK, B. L. ENGELSTAD, R. R. BACON, C. C. COMPTON, D. L. WHITE, P. JACOBS, AND J. LEWIS, *Am. J. Roentgenol.* **152,** 167 (1989).
18. A. E. MARTELL AND R. M. SMITH, "Critical Stability Constants. Vol. 3. Other Organic Ligands," Plenum, New York, 1977.
19. B. VENUGOPAL AND T. D. LUCKEY, "Metal Toxicity in Mammals. Vol. 2. Chemical Toxicity of Metals and Metalloids," Plenum, New York, 1978.
20. P. GAEHTGENS, in "Handbuch der allgemeinen pathologie. Vol. 3, 3rd Part. Mikrozirkulation" (H. Messens, Ed.), pp. 231–287, Springer-Verlag, Berlin, 1977.
21. K. R. THULBORN, J. C. WATERTON, P. M. MATTHEWS, AND G. K. RADDA, *Biochim. Biophys. Acta* **714,** 265 (1982).
22. K. J. PACKER, *J. Magn. Reson.* **9,** 438 (1973).
23. B. ROBERTSON, *Phys. Rev.* **151,** 273 (1966).
24. J. A. GLASEL AND K. H. LEE, *J. Am. Chem. Soc.* **96,** 970 (1974).